

NONLINEAR STRUCTURAL ANALYSIS OF A TURBINE AIRFOIL USING THE  
WALKER VISCOPLASTIC MATERIAL MODEL FOR B1900 + Hf

T.G. Meyer, J.T. Hill, R.M. Weber  
Pratt & Whitney  
East Hartford, Connecticut 06108

A viscoplastic material model for the high temperature turbine airfoil material B1900 + Hf has been developed under NASA contract NAS3-23925, "Constitutive Modeling for Isotropic Materials (HOST)"<sup>1</sup>, and has been demonstrated in a three dimensional finite element analysis of a typical turbine airfoil. The demonstration problem is a simulated flight cycle and includes the appropriate transient thermal and mechanical loads typically experienced by these components. The Walker viscoplastic material model was shown to be efficient, stable and easily used. The following report summarizes the demonstration analysis and evaluates the performance of the material model.

Background

In recent years unified constitutive models have been developed as alternatives to the classical elastic-plastic-creep models for modeling nonlinear material behavior. These unified models are mathematically and functionally elegant and are capable of representing material nonlinear behavior over a wide range of temperatures and loading conditions while avoiding the simplifying assumptions of classical theory. The unified models are characterized by the use of a kinetic equation to relate inelastic strain rate to the applied stress and one or more internal state variables. Evolutionary equations are used to describe the variation of the internal state variables with loading history. Models of this kind have been shown to be capable of treating all aspects of inelastic deformation including plasticity, creep and stress relaxation.

PRECEDING PAGE BLANK NOT FILMED

ORIGINAL PAGE IS  
OF POOR QUALITY

Several unified models are being evaluated in a current NASA sponsored technical program, "Constitutive Modeling for Isotropic Materials (HOST)"<sup>1</sup>. Part of the evaluation includes a demonstration in an analysis of gas turbine component under simulated flight conditions. This paper presents the results of the demonstration of one of the unified models; the two state variable model patterned after Walker<sup>2,3</sup>. In this model, the general form of the inelastic flow law relates the plastic strain rate tensor,  $\dot{C}_{ij}$ , to the applied deviatoric stress,  $S_{ij}$ , by the simple relationship:

$$\dot{C}_{ij} = f \left( \frac{S_{ij} - \Omega_{ij}}{K} \right)$$

where  $\Omega_{ij}$  represents the "equilibrium" or "back" stress; and  $K$ , a scalar quantity, represents the degree of isotropic hardening. This two state variable unified model was developed by Walker<sup>2,3</sup> and modified during the present NASA program<sup>1</sup>, and includes the increased computational efficiency features developed by Cassenti<sup>4</sup>.

#### Component Finite Element Model Description

The component chosen for the demonstration of the B1900 + Hf viscoplastic material model is the airfoil portion of a typical cooled turbine blade. The foil was analyzed using the MARC<sup>5</sup> finite element program. Figure 1 shows the finite element mesh used in the analysis. A total of 173 elements and 418 nodes were used to describe the geometry, resulting in 1086 degrees of freedom. Two element types were used in the mesh. The bulk of the airfoil was modeled using 8 noded solid elements (MARC element type 7), but a portion of the leading edge was modeled with higher order 20 noded solid elements (MARC element type 21). A total of twenty four higher order elements were used in this region.

#### Boundary Conditions and Loading

The loading and boundary conditions were chosen to simulate a typical commercial engine flight. The flight simulation is shown schematically in Figure 2 and includes periods of Taxi, Take-Off, Climb, Cruise, Descent, Taxi and finally Shutdown. The Take-Off portion includes a momentary pause in engine acceleration to more faithfully simulate actual "rolling take-off" conditions. The range of foil temperatures and the centrifugal load spectrum encompassed in the simulated flight exercises the material model over most of its range of applicability.

Radial deflections were specified to be zero at the radially innermost section of the foil. Additional nodal boundary conditions were imposed in this plane to fully suppress rigid body motion.

The flight cycle was described in the stress analysis as a series of load increments which accounted for time steps and corresponding centrifugal loads and temperature profiles which were accessed from a previously generated thermal tape. The analysis proceeded until the cyclic response of the foil was noted to be stable from one flight to the next.

To allow the possibility of a very small load increments in the stress analysis, temperature profiles were defined frequently on the thermal tape. The maximum nodal temperature change from one profile to the next was 50C. In the Take-Off portion of the flight, where foil temperatures change rapidly, 25 time points were used. During the Cruise portion of the flight, the temperature profile is essentially constant. However, the material model state variables continue to evolve ( e.g. creep deformation), so that step size is still important. Consequently, a large number of increments, (twenty-eight), were used in this portion of the flight. In total, 83 loading increments were used for each flight.

#### Stress Analysis Results; Accuracy and Stability

Two locations on the airfoil have been selected to illustrate the the results of the analysis. The behavior at these locations was expected to be very different and to provide an evaluation of the model over the widest possible range of conditions on the airfoil. Figure 3 shows the location of these points superimposed on the temperature profile during Cruise. Point A corresponds to the integration point nearest the external wall at the leading edge "hot spot", and was expected to have the largest amount of inelasticity in the foil. Point B corresponds to the integration point nearest the internal wall at an adjacent "cool spot". Both points are in the region of the model having higher order solid elements.

Figure 4 shows the strain - temperature history at the locations of interest during the first flight. The Take-Off portion is shown in more detail than the remainder of the flight. The various parts of the flight are labeled consistently with the flight definition shown in Figure 2. Figures 5 and 6 show the stress - strain response during all three flights at locations A and B respectively. The two locations present somewhat different pictures of the cyclic response: At location A, it is appears that a stablized hysteresis loop is achieved after just three flights. At the end of Take-Off, the largest variation in stress or strain between the second and third flights is

less than 2% ( see Table 1 ) and this is much less than the change between the first and second flight. However at location B the change between successive flights is decreasing less rapidly ( 5% and 4% ). Thus the analysis predicts that different parts of the foil stabilize at different rates, which is reasonable since the loading and temperatures vary significantly from one location to another. In an actual airfoil it could be expected that the cyclic response from one flight to the next may be very similar even though it may never completely "stabilize" due to load redistribution from adjacent sections. As a result the hysteresis loop at any location may ratchet throughout the service life. Consequently, it is not appropriate to judge the material model stability based on the stress - strain response alone. More useful criteria are those of smoothness and sensitivity to step size. The stress - strain response in Figures 5 and 6 shows no tendency to severe oscillation. The "looping" observed during initial loading at location A is a result of the complex thermal and mechanical loading on the foil during the "rolling take-off" portion of the flight and should not be interpreted as of a material model deficiency.

Table 1

Change in stress and strain from one flight to the next

Values at the end of Take-Off

Flight	Stress (MPa)	Strain (%)	Inelastic Strain (%)
At Location A			
1st	-235.9	-0.339	-0.239
2nd	-213.1	-0.344	-0.267
3rd	-209.7	-0.343	-0.276
At Location B			
1st	629.7	0.365	0.068
2nd	594.5	0.371	0.096
3rd	569.0	0.376	0.119

Additional insight regarding the behavior of the material model and the adequacy of the solution can be gained by examining the evolution of key state variables and the inelastic strains. Figure 7 shows the evolution of the back stress in the radial direction at locations A and B during the first flight. Once again, the Take-Off pause is easily identified. The evolution of the inelastic strain in the radial direction during the first flight is shown in Figure 8 for

location A. It is clear that these variables evolve smoothly, adding confidence in the behavior of the model and the fidelity of the analysis.

Figure 8 shows the accumulation of inelastic strain at location A during all three flights. Several observations can be made. First, the bulk of the inelastic strain is accumulated during Take-Off on the first flight. Secondly, the element exhibits some degree of reversed inelasticity as evidenced by the decrease in the inelastic strain during Cruise and Descent. The Take -Off portions of the second and third flights have nearly the same amounts of inelastic strain accumulation, indicating that the overall hysteresis loop shape is essentially unchanged.

A further check on the model can be made by checking that the effective stress and effective strains during initial stages of loading coincide with the normal monotonic tensile behavior. This check is valid only during early stages of loading before significant inelastic history has been accumulated. This check was made for location A at increment 19 which shows the first significant amount of inelastic strain. At increment 19, the inelastic strain is approximately 10% of the total mechanical strain. On the previous increment the inelastic strain was only 4% of the total strain. Figure 9 shows the monotonic stress - strain curve predicted by the material model (at a temperature and strain rate consistent with increment 19) along with the effective stress/ effective strain calculated for that increment.

#### Sensitivity to Step Size and Efficiency

A study was conducted to determine the sensitivity of the solution and material model behavior to step size. The results reported above, (Base Case), were obtained using 23 increments to describe the Take-Off portion between ground Idle and the end of Take-Off. In this study, this same period was described in 10 increments, (Case 2), and in 6 increments, (Case 3). Only the first flight was studied. Figure 10 shows the resulting stress - strain response at location A. Case 3 failed to converge to a solution on increment 8. The convergence failure occurred at an element other than location A. Case 2 converged for all increments and produced results at the end of Take-Off which are in very good agreement with the Base Case.

It should also be noted that the improved efficiency integration techniques introduced by Cassenti<sup>4</sup> resulted in very fast solution times for the nonlinear analysis. Computing times for the nonlinear analysis were compared to computing times for a conventional elastic analysis at various times in the flight cycle. It was found that the

matrix solution times were the same, indicating that the material model routines are very efficient. The efficiency measures developed by Cassenti avoid matrix inversion on each increment. Instead, the stiffness matrix is assembled at a reference temperature only, and any change in the stiffness due to temperature dependent elastic properties is passed to the main MARC program as an incremental inelastic stress vector. The reference temperature stiffness matrix is assembled only at the start of the inelastic analysis and each time the inelastic analysis is restarted. The net effect is that an inelastic analysis involving several increments actually uses less computing time than an equal number of separate elastic analyses, because each separate elastic analysis requires the stiffness matrix to be assembled anew.

### Conclusions

The two state variable (Walker) viscoplastic model for B1900 has been successfully demonstrated in an analysis of a turbine airfoil under complex and realistic flight cycle loading. The model behaved very stably throughout the flight cycle, was easily used and is very efficient. Each inelastic solution is no more expensive than an elastic solution. The model was demonstrated using both linear strain and higher order three dimensional elements. A sensitivity study indicates that surprisingly large time/temperature/load steps could be used.

### References

1. Constitutive Modeling for Isotropic Materials (HOST), NASA3-23925.
2. Walker, K.P., "Research and Development Program for Nonlinear Modeling with Advanced Time-Temperature Dependent Constitutive Relationships", Final Report, NASA CR-165533.
3. Walker, K.P., "Constitutive Modeling of Engine Materials", Final Report FR-17911, AFML Contract F33615-81-C-5040, November 1983.
4. Cassenti, B.N., "Research and Development Program for Nonlinear Structural Modeling with Advanced Time-Temperature Dependent Constitutive Relationships, Vol. I - Theoretical Discussion." Final Report NASA CR168191, July, 1983.
5. MARC General Purpose Finite Element Program, MARC Corporation, Palo Alto, Ca.

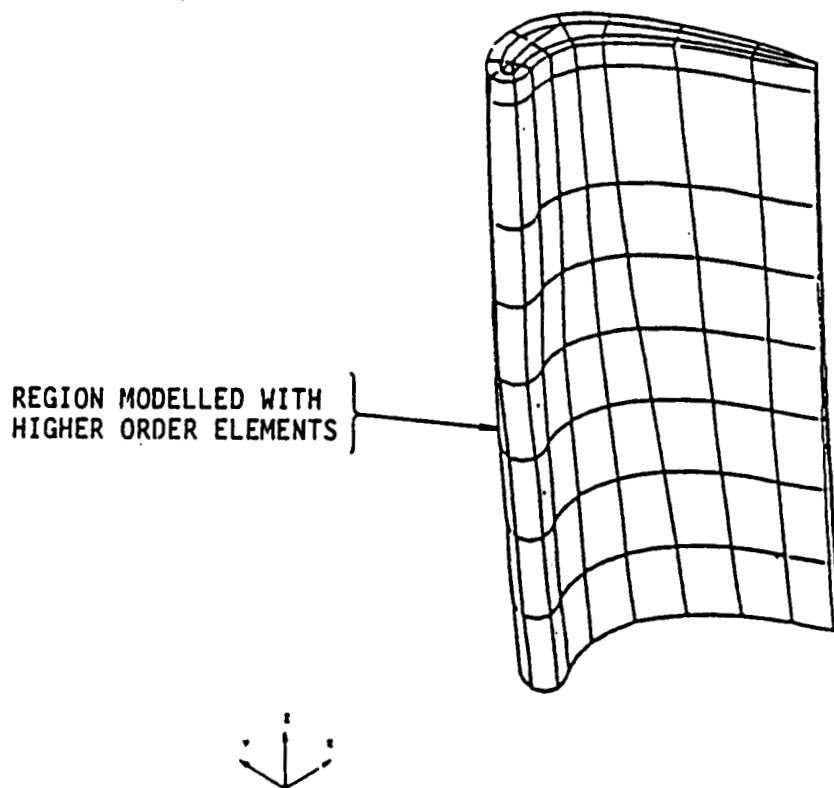


Figure 1. Finite Element Mesh Used for Constitutive Model Demonstration

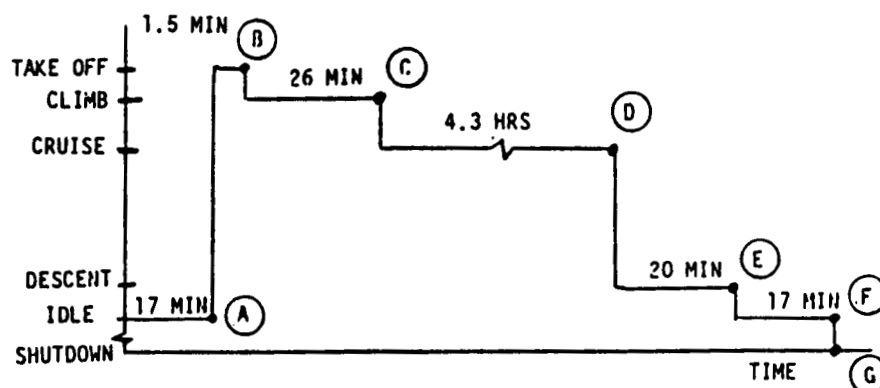


Figure 2. Simulated Flight Used in The Demonstration Analysis

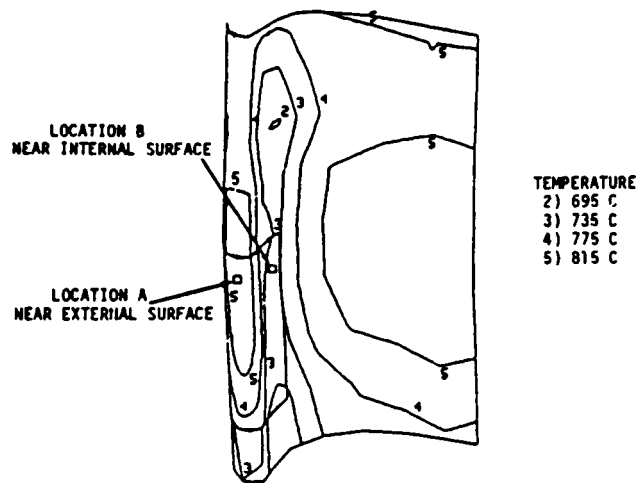


Figure 3. Steady State Temperature Profile During Cruise and Locations A and B Examined in Detail

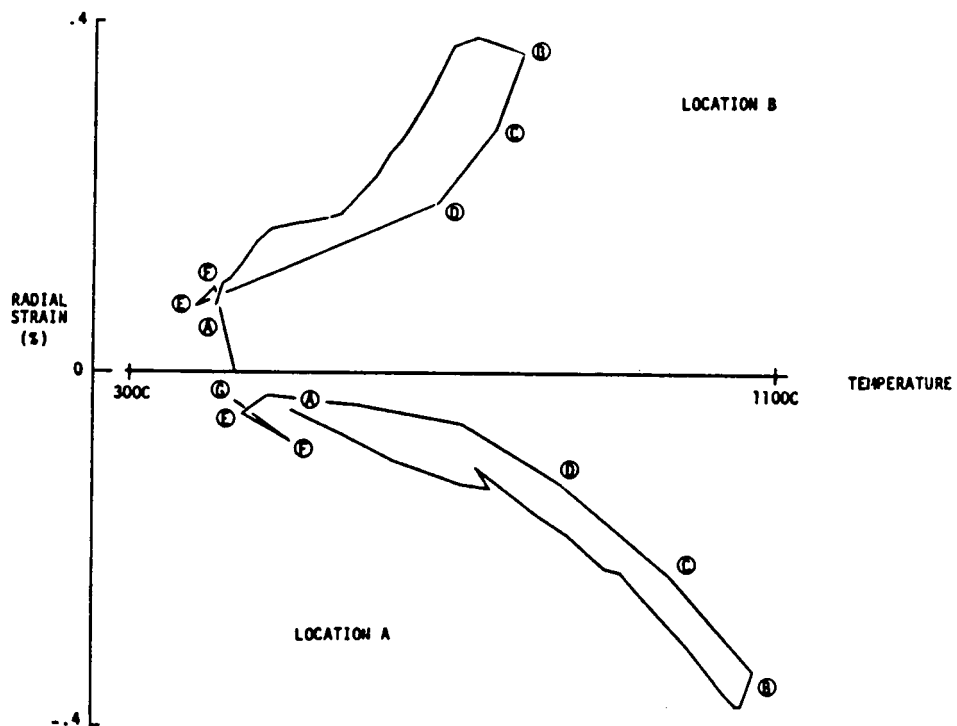


Figure 4. Strain-Temperature History at Locations A and B During First Flight

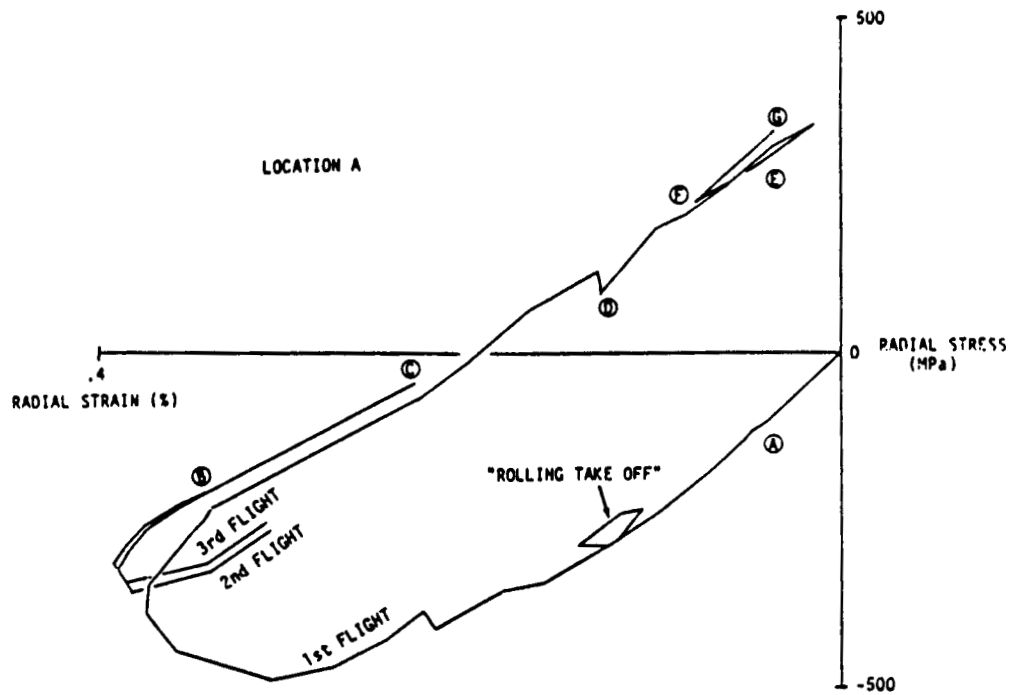


Figure 5. Stress-Strain Response at Location A

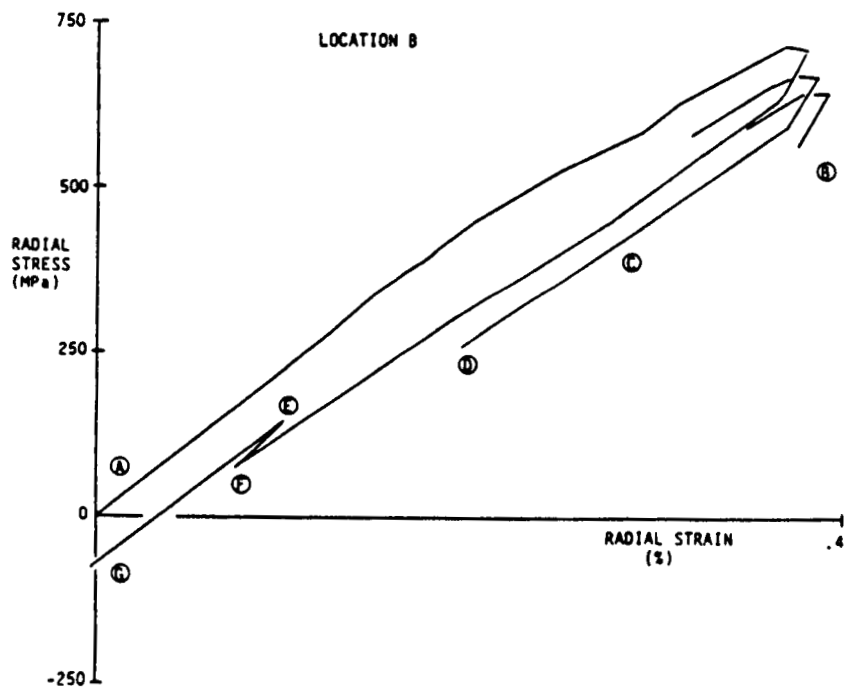


Figure 6. Stress-Strain Response at Location B

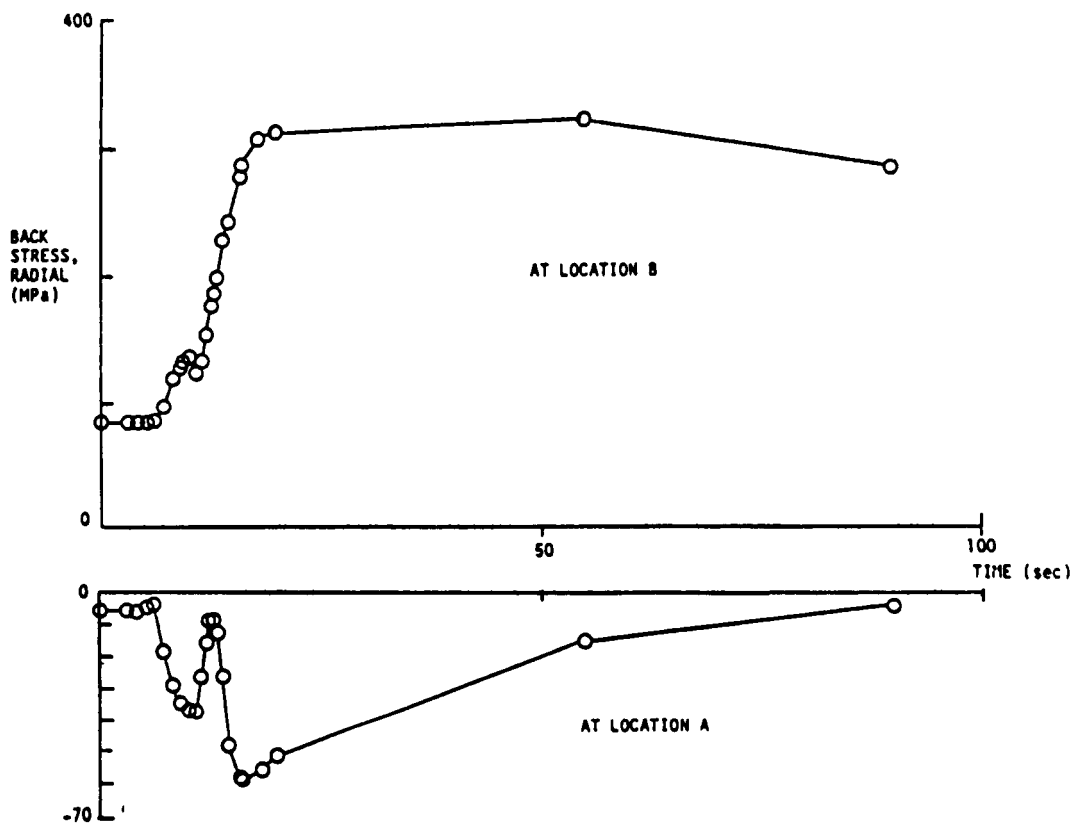


Figure 7. Evolution of Back Stress During Take-Off in the First Flight

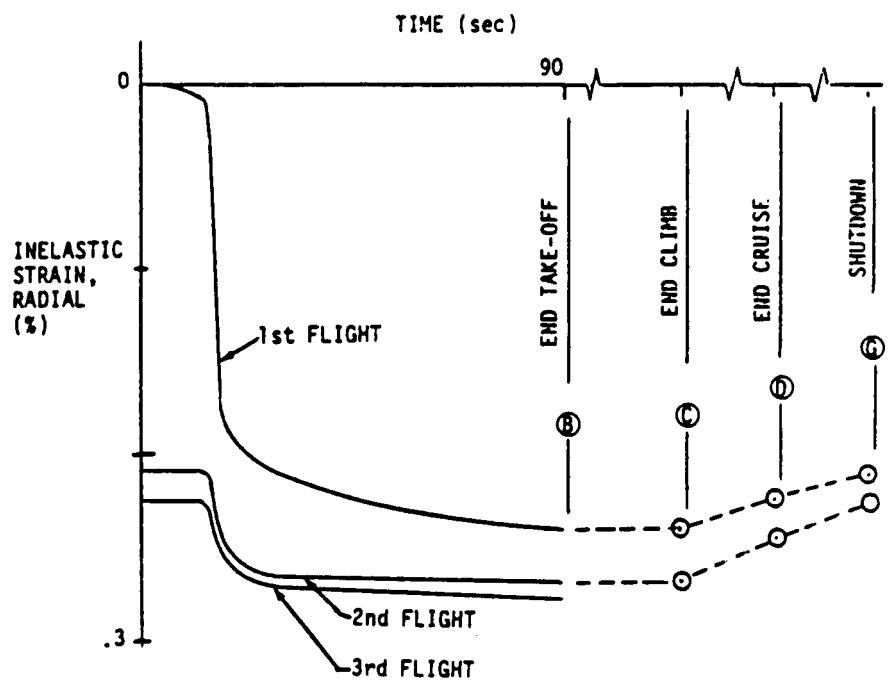


Figure 8. Accumulation of Inelastic Strain at Location A During Three Flights.

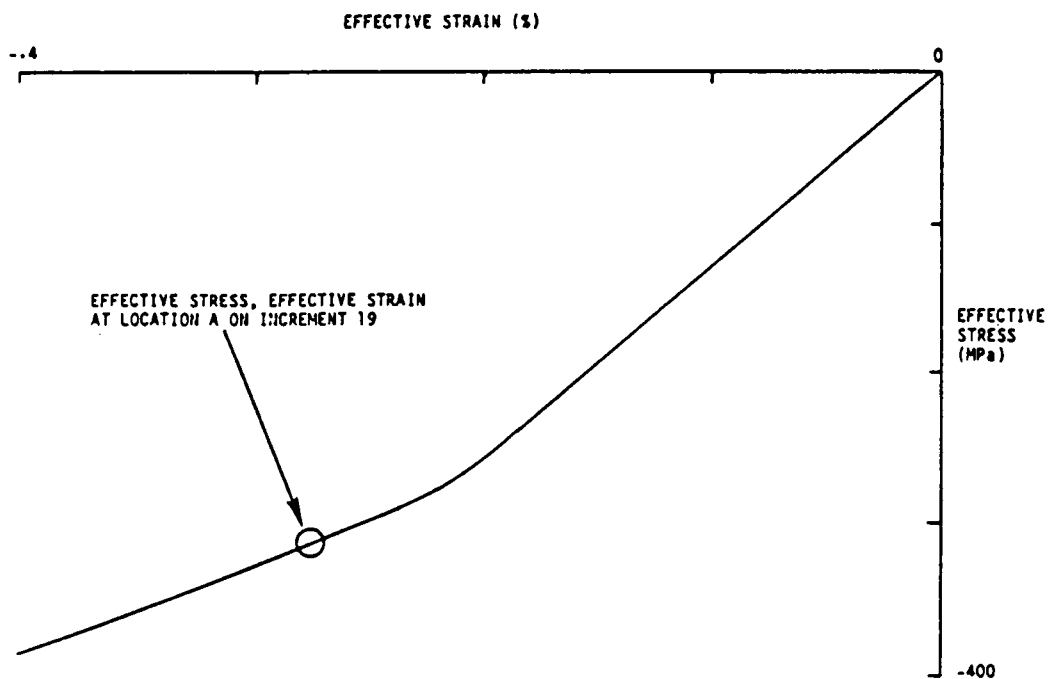


Figure 9. The Effective Stress/Effective Strain at Location A Follows the Expected Monotonic Curve.

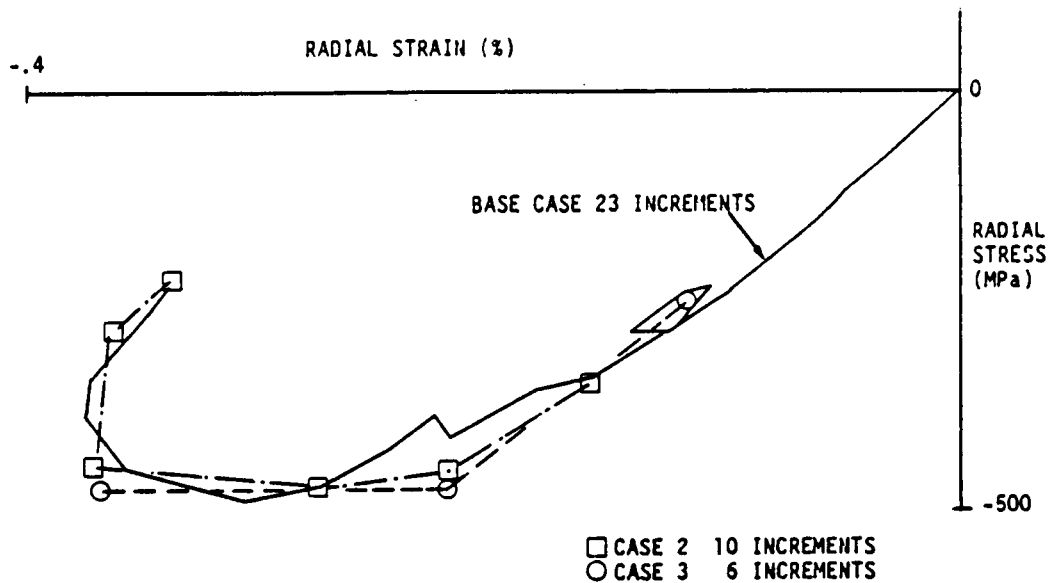


Figure 10. Effect of Step Size During Take-Off of the First Flight